Theor Chem Acc (2007) 117:755–764
DOI 10.1007/s00214-006-0206-1

REGULAR ARTICLE

Non-stationary states in chemistry

Alessandro Lami · Giovanni Villani

Received: 9 June 2006 / Accepted: 13 October 2006 / Published online: 9 January 2007

Abstract After a brief introduction to the theoretical area concerning the propagation of non-stationary states, two examples of our activities in the field of time-dependent processes are presented and discussed. The first concerns the possibility of controlling photochemical and photophysical processes by properly shaped, short, weak laser pulses. A theoretical approach developed by our group is briefly reviewed and a new example is presented on the control of the energy deposition in a model linear aggregate of ten chromophores. The second example deals with hydrogen transfer in DNA base pairs and presents the result of a time-dependent calculation on adenine–thymine and guanine–cytosine pairs. These calculations show a coherent, periodic behaviour and make it evident that imino-enol tautomerism cannot be interpreted as a source of mutations, since it would generate too many mutation points along the DNA.

Keywords Time-dependent processes · Non-stationary states · Laser control · Imino-enol tautomerism · A–T and G–C base pairs

1 Introduction

The time-dependent Schrödinger equation (TDSE) has been considered for a long time a secondary subject in standard textbooks on Quantum Chemistry. In practice, it was introduced just to derive the expression for the transition probability of a molecule, subject to a weak oscillating electric field, by the first order perturbation theory. The focus was mainly on the development of suitable methods for the calculation of eigenstates and eigenvalues of the molecular Hamiltonian, since the time-dependent behavior was considered just a matter of multiplying each term of the expansion in term of eigenstates by the right time-dependent phase factor $\exp(-iE_j t)$. The alternative way of looking directly at the dynamical problem has been scarcely pursued in the conviction that basically no molecular process could be detected in the time domain for lack of suitable instruments.

This double way of looking at the time-behavior of quantum states is well illustrated by the elementary, but instructive, example of the motion of a coherent state of the harmonic oscillator.

The wave-function for the ground state displaced at x_0 is

$$\psi(x_0) = \mathrm{N} \mathrm{e}^{-\frac{\mathrm{m}\omega}{2}(x-x_0)^2} \tag{1}$$

and its time evolution can be written down as:

$$\begin{aligned}\psi(x_0,t) &= \sum_n |\chi_n\rangle \langle\chi_n \mid \psi(x_0)\rangle \, \mathrm{e}^{i(n\omega+1/2)t/\hbar} \\ &= \mathrm{e}^{-\frac{m\omega}{4}x_0^2} \sum_n \frac{1}{\sqrt{n!}} \left(\frac{m\omega}{2}x_0^2\right)^n \mathrm{e}^{i(n\omega+1/2)t/\hbar} \, |\chi_n\rangle \,,\end{aligned} \tag{2}$$

where the last passage requires a few algebraic manipulations.

The alternative way is to solve directly the TDSE:

$$i\frac{\partial\psi}{\partial \mathrm{t}} = H\psi. \tag{3}$$

A. Lami (✉) · G. Villani
Istituto per I Processi Chimico-Fisici (IPCF) del CNR,
Via G. Moruzzi 1, 56124 Pisa, Italy
e-mail: lami@ipcf.cur.it

Starting with the trial function:

$$\psi(x,t) = \exp\left(-\frac{m\omega}{2}(x - X(t))^2 + iP(t)\right) \tag{4}$$

and substituting in Eq. (3), one finds that $X(t)$ and $P(t)$ define the classical phase–space trajectory (starting at x_0 with null momentum). One may of course demonstrate that the two results are completely equivalent. In the first, the right time evolution is obtained through the interference of eigenstates, while in the second, one gets a more transparent result, showing clearly the similitude with the classical dynamics. Moreover, the second approach can be considered as the starting point of the very fruitful approximate method developed by Heller [1–3].

Things changed radically with the parallel development of pulsed lasers and of detection devices with a time resolution of a few femtoseconds, which opened the way to modern femto-chemistry. The development of methods for the numerical solution of TDSE became a necessary step for interpreting a lot of time-resolved experimental data as well as for looking at elementary chemical processes under a new perspective. In the last few years, various eigenstate-free approaches have been developed for investigating the behavior of non-stationary states as semiclassical propagators [4–6], Lanczos propagation of TDSE [7–10] and multi-configuration time-dependent Hartree methods (MCTDH) [11–13]. While on the one hand it is in fact clear that the information content of a purely dynamical calculation (i.e. eigenstate-free) involving longtime propagation is identical to the one involving the eigenstates expansion, on the other hand, in many cases, it is the short-time behavior that is important for practical purposes and an approach pointing directly to TDSE is much more economical. This is well illustrated by the problem of the computation of the absorption bandshape for a molecule (linear response). The spectrum can be conveniently evaluated as the Fourier transform of the dipole autocorrelation function:

$$\begin{aligned} A(\omega) &\propto \int \exp(-i\omega t)\ \langle g|\, \mathrm{d}(t)\, d\, |g\rangle\, \mathrm{d}t \\ &= \int \exp(-i(\omega - E_g)t)\ \langle g|\, \mathrm{d}\, U(t)\ d\, |g\rangle\, \mathrm{d}t. \end{aligned} \tag{5}$$

The latter is obtained by propagating the doorway state $d\,|g\rangle$. If one deals with a high-resolution spectrum of a nearly isolated molecule, a longtime propagation is needed to reproduce fine frequency details, and the effort of the time-dependent approach becomes comparable to that of computing the eigenvalues of the Hamiltonian. If one is interested in a condensed phase spectrum, then the time-dependent approach becomes much more convenient, since the various broadening mechanisms damp the integrand of Eq. (5) in such a way that only a short-time numerical propagation of the doorway state is needed.

Since a non-stationary state is a coherent superposition of energy eigenstates, it can be prepared only by a coherent broad-band light source, i.e. by a laser pulse. As an example, let us consider a Gaussian laser pulse containing a single carrier frequency ω (E is the electric field):

$$E(t) = E_0 \cos(\omega t + \phi)\ \exp(-(t - t_c)^2/\,\Gamma_t^2). \tag{6}$$

Its Fourier transform is

$$E(\omega) \propto \mathrm{E}_0 \exp(-(\Omega - \omega)^2/\,\Gamma_\omega^2); \qquad \Gamma_\omega^2 = 2/\,\Gamma_t^2. \tag{7}$$

Thus, if $\Gamma_t = 20$ fs, then, according to Fourier analysis, $\Gamma_\omega = 2,124\,\mathrm{cm}^{-1}$, which means that the excitation band covers a few thousand cm^{-1} (i.e., usually, a single excited electronic state but many vibro-rotational states). As previously discussed, one may look at the motion of the excited nuclear wave-packet as a quantum trajectory on the potential energy surface or as the result of a complex interferential pattern between eigenstates.

The above consideration introduces the last point we want to make in this introduction. In the whole realm of time-dependent phenomena, one has to deal with the corner-stone of Quantum Mechanics, i.e. the superposition principle with its paradoxical aspects. The evolving state may in fact be a linear combination of states of very different nature, thus recalling Schrödinger cat states, as for example in symmetric mixed-valence compounds in which one excess electron is simultaneously on each moiety [14], or during light absorption, when the molecule is simultaneously in the ground state and in the excited state. These peculiar quantum features, which have attracted a renewed interest in the last few years for the exciting theoretical possibility of building up quantum computers [15–18], are however very fragile with respect to the decoherence due to the system–surrounding interaction. In practice, it happens that after a few femtoseconds from its creation in a linear superposition state, each molecule will be forced to choose among one of its component states and thus behave as a classical object in this respect [19]. If we deal with N molecules, this decoherence is further accelerated by the fact that they are normally prepared in slightly different non-stationary states, and thus after a certain time the different phase evolution will determine per se an incoherent response. The maintenance of coherence is, in fact, a huge problem to be solved in order to take practical advantage of the quantum computing idea.

After this short introduction, we move to concrete examples, presenting a few selected results obtained recently by our group, which has been working for several years [20,21] in the area of theoretical study of time-dependent phenomena in molecules and aggregates. These concern the problem of achieving some control of molecular processes occurring in excited states through suitably shaped laser pulses (Sect. 2) and the modeling of proton transfer in DNA (Sect. 3).

2 The weak-field control

The idea of controlling molecular processes by laser pulses dates a long time back [22,23]. It is however only in recent years that efficient experimental setups have been realized based on the development of the ultrafast pulse shaping techniques [24]. Basically, the laser pulse is first separated into its monochromatic components, which are then forced to travel through different liquid crystal pixels and them recombined to give the shaped field. A computer-assisted modification of the local electric field acting on each pixel changes the optical path in such a way that the right phase and amplitude of each component is achieved. As a further step, the pulse shaper may be coupled to the instrument measuring the observable, one is interested in, to build up a system capable of achieving the required optimal result through a computer-guided self-learning algorithm [25,26].

An exposition of the general mathematical theory of the control applied to the quantum system may be found, for example, in Ref [22,23]. Our interest has been directed to the weak-field approximation, which is not only much simpler from the mathematical point of view, but also more physically transparent [27–30]. One of the problems in this field is that one can obtain a good result without any idea of the reasons why a given shaped pulse works.

In order to illustrate how things go, let us consider what happens when a multilevel system, initially in its ground state, is perturbed by a weak multicolor Gaussian laser pulse:

$$E(t) = \sum_j E_{0\mathrm{j}} \cos(\omega_j t + \varphi_j) \exp(-(t - t_\mathrm{c})^2 / \Gamma_t^2) = \sum_j \exp(-(t - t_\mathrm{c})^2 / \Gamma_t^2)\,(z_j \exp(-i\omega_j t) + c.c.), \quad (8)$$

where phases and real amplitudes are grouped in the complex amplitudes $z_j = E_{oj} \exp(-i\phi_j)$.

The total Hamiltonian is written as

$$H = H_M + V(t), \quad (9)$$

where:

$$H_M = E_g \,|g\rangle\,\langle g| + \sum_m E_m \,|m\rangle\,\langle m| \quad \text{and}$$

$$V(t) = -E(t) \sum_m (\langle g|\, d\, |m\rangle\ |g\rangle\,\langle m| + h.c.). \quad (10)$$

(H_M is the molecular part, $V(t)$ the field–molecule interaction and $\langle g|\, d\, |m\rangle$ are the dipole matrix elements between the ground state and the various excited states (the excited state–excited state dipole elements are supposed to be null here).

The TDSE is solved using the first-order time-dependent perturbation theory. After a few straightforward passages and using the rotating-wave approximation, one arrives at the following form of the excited-state part of the evolving state at time t (after the end of the pulse), showing explicitly the dependence on phase and amplitudes (N is a normalization constant):

$$|\psi_e(t)\rangle = N \sum_m c_m \exp(-i * E_m t)\,|m\rangle, \quad (11)$$

where the vectors of coefficients and complex amplitudes, $\mathbf{c}$ and $\mathbf{z}$ respectively, are linearly related:

$$\mathbf{c} = \mathbf{A}\,\mathbf{z} \quad (12)$$

and

$$A_{mj} = \sqrt{\pi}\,\Gamma_t \,\langle g|\, d\, |m\rangle\ \exp(-\Delta_{mj}(\Gamma_t^2 \Delta_{mj} + 4it_p)/4),$$
$$\Delta_{mj} = E_g + \omega_j - E_m. \quad (13)$$

We could be interested in the mean value of the given observable or in a quantity that depends on the whole history, as, for example, the total energy absorbed or emitted coherently by the molecule (this last is due to the fact that for the whole time interval in which the system is in a linear combination involving the ground state and the excited states, the mean value of the dipole oscillates and thus, according to Maxwell equation, it radiates). In any case, our task is to find the absolute maximum (minimum) of a function $F_\alpha(\mathbf{E_0}, \boldsymbol{\omega})$ of phases and amplitudes, which are the control parameters (the carrier frequencies will be held as constant). The total energy carried by the pulse must be obviously taken as a constraint to avoid trivial solutions (e.g., we could increase a given observable concerning excited states by simply increasing the field strength). The above is not in general an easy problem, from a numerical point of view, since the modeling of a realistic system involves many states and thus the surface $F_\alpha(\mathbf{E_0}, \boldsymbol{\omega})$ has many maxima and minima. Specific algorithms, such as the genetic one [31], have been developed for such a purpose, but their application may be time consuming for large systems [28].

Another important point to be considered is the one concerning the stability of the solution we obtain. In fact, one should not forget that, since amplitudes and phases can be experimentally controlled only with a certain degree of approximation, the final result is physically significant only if it remains stable while the control parameters are allowed to vary within the experimental error. In order to illustrate this point, it is useful to see what happens if we decide that our goal is to prepare at time t a non-stationary state, whose excited state component is assigned:

$$|\chi_e(\mathrm{t})\rangle = \sum_m v_m \mathrm{e}^{-iE_m t} |m\rangle. \tag{14}$$

From Eqs. (11), (12) and (14) it is clear that the problem translates into the linear system:

$$\mathbf{v} = \mathbf{A}\,\mathbf{z}, \tag{15}$$

which is determined after selecting a number of complex amplitudes (i.e of carrier frequencies) equal to the number of $|m\rangle$ states.

Applying Eq. (15) to several model Hamiltonians, we have verified that very often the matrix $\mathbf{A}$ has a certain number of eigenvalues whose absolute value is very small. Hence its inversion is a source of instability, meaning that a small error in the choice of phases and amplitudes may give rise to a state, which at time t is very different from the goal, Eq. (14).

In order to overcome this problem, we have developed and applied a procedure grounded on the linearity introduced by the weak field assumption. The above means that to each pulse, like the one in Eq. (8), is associated a different prepared state, while a linear combination of pulses gives rise to the corresponding linear combination of excited states (only real coefficients are considered since the electric field is real). Let us first select a linear space of pulses (whose dimension is N_p) in which to search the optimal one and the corresponding linear space of prepared states (see below). A generic pulse can be written as

$$\mathrm{E}(\mathrm{t}) = \tilde{\mathbf{x}}\,(\mathbf{Z}\,\boldsymbol{\Omega}(\mathbf{t}) + \mathbf{c.c}). \tag{16}$$

Here, $\mathbf{x}$ and $\boldsymbol{\Omega}$ are column vectors whose dimensions are N_p and N_m (the number of $|m\rangle$ states) respectively; the real vector $\mathbf{x}$ gives the coefficients of the linear combination, while $\boldsymbol{\Omega}_j = \mathrm{e}^{-i\omega_k t}$.

The $\mathbf{z}$ vectors specifying the pulses selected as basis are the columns of the matrix $\mathbf{Z}$. The total energy carried by the pulse can be compactly written as

$$E_P = \tilde{\mathbf{x}}\,\mathbf{W}\,\mathbf{x}, \tag{17}$$

where, as shown in Ref. [29], $\mathbf{W}$ is a matrix that can be easily built up from the selected pulses.

If $|\mathbf{R}\rangle$ is the row vector of the states prepared by the pulses chosen as the basis set, then the state prepared by the pulse (16) is $|u\rangle = |\mathbf{R}\rangle\ \mathbf{x}$, while the mean value of a given observable O is

$$\langle O\rangle = \tilde{\mathbf{x}}\ \langle\mathbf{R}|\,O\,|\mathbf{R}\rangle\ \mathbf{x} = \tilde{\mathbf{x}}\,\mathbf{O}\,\mathbf{x}. \tag{18}$$

Our variational problem is then:

$$\delta(\tilde{\mathbf{x}}\,\mathbf{O}\,\mathbf{x} - \lambda\,\tilde{\mathbf{x}}\,\mathbf{W}\,\mathbf{x}) = 0, \tag{19}$$

leading to the following eigenvalue problem for a non-symmetric matrix:

$$(\mathbf{W^{-1}}\,\mathbf{O})\,\mathbf{x} = \lambda\,\mathbf{x}. \tag{20}$$

The eigenvector corresponding to the maximum eigenvalue gives the optimal linear combination of the selected pulses (the minimum is chosen if one wants to minimize something). In practice, our method can be summarized in the following points.

(1) We select a certain number of carrier frequencies covering the absorption band. These do not vary in the optimization (i.e. one works only on complex amplitudes).
(2) We then perform a sequence of steps, generating a random amplitude and phase for each frequency component. A check is performed after each step to verify if the prepared state is linearly independent of the previous ones. Only in the positive case, the generated pulse is accepted and memorized together with the corresponding state. In practice, we just look at the smallest eigenvalue of the tentative new overlap matrix and accept the pulse only if it is above a given threshold. This ensures a certain degree of stability to the solution, which can be further enforced, as discussed in Ref. [27,28]. After a fixed, large number of unfruitful trials to enlarge the linear space, the procedure is stopped.
(3) The final step is to solve the variational problem in the selected linear space, building up the matrices $\mathbf{W}$ and $\mathbf{O}$ and solving Eq. (20).

It is clear from the previous points that the whole procedure can be performed also in an eigenstate-free context. In other words, it does not matter if the Hamiltonian is written, as usual, in terms of coordinates and momenta; what is important is our ability to solve the time-dependent Schroedinger equation for the system weakly perturbed by the light pulse.

Various cases have been treated by the method described above, which shows its ability to achieve some control of the dynamics of complex systems exhibiting conical intersections. In Ref. [27], we studied a model system with two harmonic diabatic surfaces coupled

to give rise to a conical intersection and showed that the pulse can be shaped to increase significantly the population of a given diabatic state at the end of the pulse. In Ref. [28], we studied the X_2A'/A_2A' conical intersection in the NO_2 molecule showing that its time-dependent fluorescence may be controlled. Different applications concern the control of the yield of competing dissociative channels on a model potential energy surface with two degrees of freedom (not published) as well the enhancement of the coherent fluorescence (free-induction decay) from the B850 ring of chromophores present in the light-harvesting 2 (LH2) complex of the purple bacterium *Rhodopseudomonas acidophila* [29]. For this case, we also generalized our method to cases in which a significant dephasing is present, working in the Liouville space.

Here, a new example is presented illustrating the possibility of controlling the energy deposition in a linear aggregate of 10 chromophores, with a nearest-neighbor exchange interaction, described by the Frenkel exciton Hamiltonian:

$$H = E_g \left|g\right\rangle \left\langle g\right| + \sum_m E_m \left|m\right\rangle \left\langle m\right| + \beta \sum_{m=1}^{9} (\left|m\right\rangle \left\langle m+1\right| + h.c.). \quad (21)$$

We have choosen here, $E_g - E_m = 11{,}345\,\mathrm{cm}^{-1}$ and $\beta = 240\,\mathrm{cm}^{-1}$. Figure 1 shows the results obtained in our attempt to optimize the excitation of terminal chromophores (more exactly, the target function is the fraction of the excited population in the two terminal chromophores) at a time of 130 fs from the pulse maximum (the caption contains further details). The comparison with the result obtained using a monochromatic Gaussian pulse with the central carrier frequency shows that the method is quite efficient also working with only five carrier frequencies. The interference between the various components gives to the optimized pulse the characteristic form shown in Fig. 2, as a function of time. A more complete analysis can be performed using the Husimi distribution illustrating simultaneously the behavior in time and frequency [29]. It is interesting to note from Fig. 2 that while the optimization is performed at time $t = 200$ fs, the fraction of excited population on the terminal chromophore remains higher, on an average, well after. Figure 3 reports the time-dependent population of the first (and of the last) chromophore in the linear chain, for the same calculation of Fig. 2. showing that despite the weak-field assumption, it is possible to have

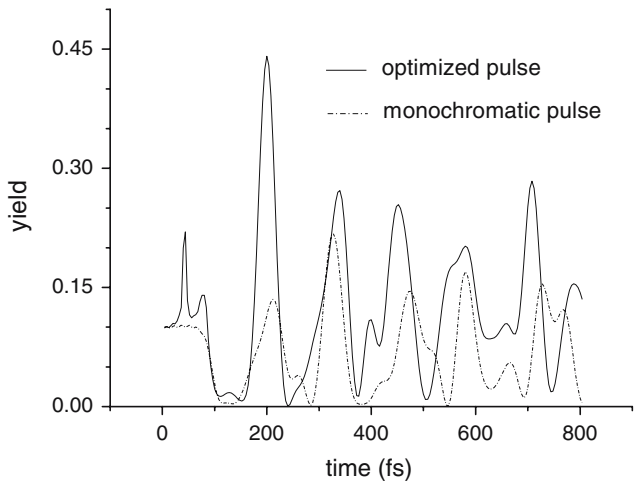

Fig. 1 The fraction of the excited population staying on the first chromophore (or on the last, identical in symmetry) as a function of time. The excitation is produced by a pulse shaped to maximize such yield at 200 fs

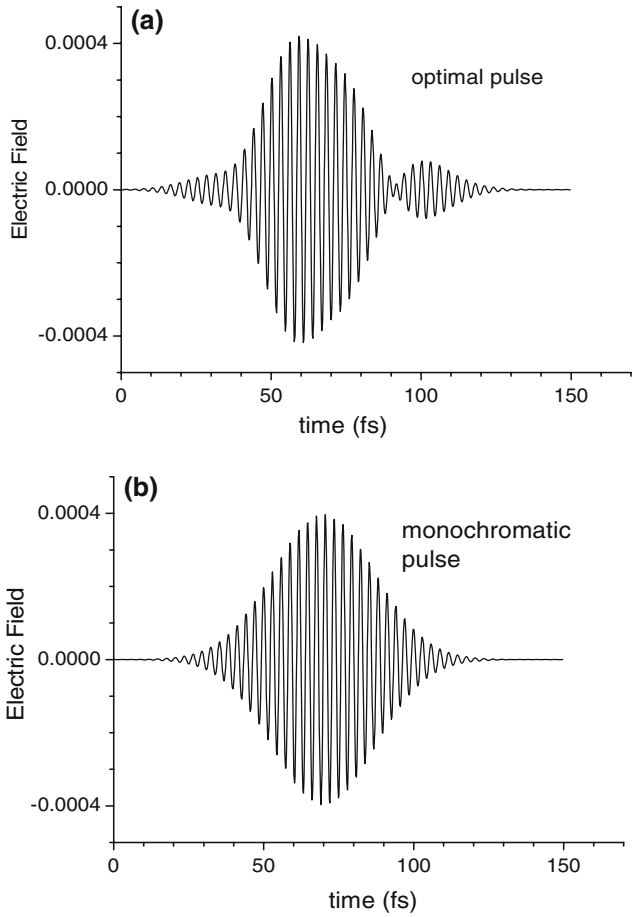

Fig. 2 **a** The optimal pulse designed for the energy deposition on the terminal chromophores of the 10-unit aggregate described by the model Hamiltonian (21). The parameters appearing in the gaussian in Eq. (8) are: $t_c = 70$ fs, $\Gamma_t = 24$ fs, while the five carrier frequencies range uniformly from 10,945 to 11,745 cm^{-1}. **b** The monochromatic pulse with a single carrier frequency of 11,345 cm^{-1}. For both (**a**) and (**b**), the fields are in atomic units

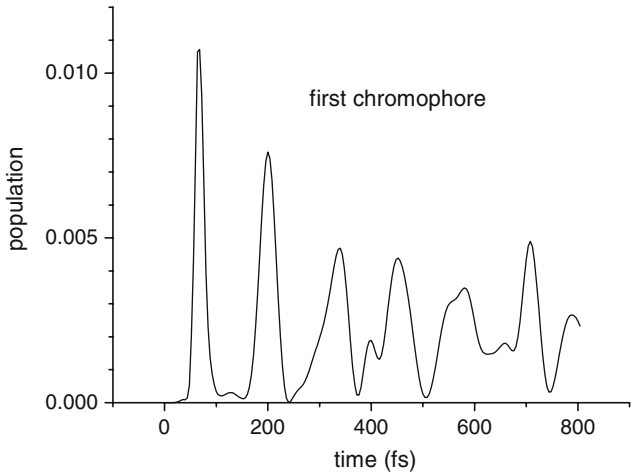

Fig. 3 The excitation probability for the first chromophore (i.e. one half of the total probability of the exciting terminal chromophores) assuming that the transition dipoles are 1 atomic unit, while the pulse is that in Fig. 2a. Due to the weak fields involved, the same curve is obtained if the transition dipoles are multiplied by a given factor while the electric field is divided by the same factor

simultaneously selectivity (as illustrated in Fig. 2) and a quite consistent degree of excitation (nearly 1% of excited aggregates).

3 A biological example: DNA dynamics

In DNA, the bases are involved in two qualitatively different mutual interaction types, hydrogen bonding and base stacking, and it is well known that these two major factors contribute to the stability of the DNA double helix. The role of hydrogen bonds is well known for providing structure and directionality in the DNA base pairs. Base stacking interaction is one of the driving forces responsible for the stabilization of the three-dimensional structure of DNA and RNA molecules. Very few studies are present in literature to directly connect these two processes [32,33] and only a paper by one of us [34] has considered the time–dependent interaction among base pairs in a quantum approach.

In the A–T case, there are two parallel hydrogen bonds and in the guanine–cytosine system, three. The most stable structure is named Watson–Crick tautomer (G–C and A–T, Fig. 1). From this structure, while keeping each monomer in its neutral form, a double hydrogen atom transfer, as proposed by Löwdin [35,36], gives the imino-enol tautomer A*–T* and G*–C* and the imino-enol-imino-enol $G^{\#}-C^{\#}$, in adenine–thymine and guanine–cytosine base pairs respectively (Fig. 4).

The idea that imino-enol tautomeric forms of DNA bases play a role in mutagenesis was formulated a few year after the Watson–Crick DNA structure [37]. If it exists an equilibrium in the two tautomeric forms of the base pair and if the rare tautomer remains stable during the time period needed for the replication process, double hydrogen transfer would play an important role in the occurrence of spontaneous mutations. Up to now, the question of whether point mutation could be formed spontaneously via the tautomerisation process remains unanswered. We believe that this is a typical problem, where a theoretical approach supported by reliable calculations can be very useful.

In a hydrogen-bonded system, a quantitative evaluation of the hydrogen transfer probability needs knowledge of the potential energy surface (PES) along the coordinates involved in this process. As demonstrated by Florián et al. [38], the use of an adiabatic potential allowing geometry relaxation during the hydrogen transfer process is also necessary to estimate both the amount of the two tautomers and the dynamics of the process. In our calculations of the electronic structure of the adenine-thymine and guanine-cytosine base pairs (performed by DFT-b3lyp with the cc-pVDZ basis set) [39,40] we have found two static stable structures for both systems: the A–T and A*–T* tautomers with an energy difference of 12.9 kcal/mol and the G–C and G*–C* tautomers with an energy difference of 8.83 Kcal/mol. Despite the fact that there are not minima corresponding to the zwitterionic structures and to the $G^{\#}$–$C^{\#}$ tautomer, these tautomers play a role in the dynamics. Dynamical calculations on these systems have been performed propagating an initial state by the Lanczos scheme (with Householder reorthogonalization) described in previous papers [9,41]. The basis set has been formed by tensorial product of the eigenstates of the three anharmonic oscillators for G–C and two for A–T base pairs. These eigenstates have been computed with an accurate numerical procedure based on a linear variational approach with a Gaussian basis set [42]. The initial state is the tensorial product of the two (or three) ground states of the monodimensional oscillators. These initial states have the same hydrogen bond situation the ground states of the Watson–Crick tautomers (A–T and G–C).

For discussing a possible mechanism leading from the Watson–Crick as to the imino-enol tautomers, we note that not all the hydrogen bonds have the same behavior. In fact in the case of adenine-thymine system, the PES as a function of the hydrogen position in the N–O bridge coordinate is steeper than that in the hydrogen position in the N–N bridge coordinate. We propose to call N–H–O *the hard hydrogen bond*, where the position of hydrogen is practically frozen, and N–H–H *the soft hydrogen bond*, where the position of hydrogen can

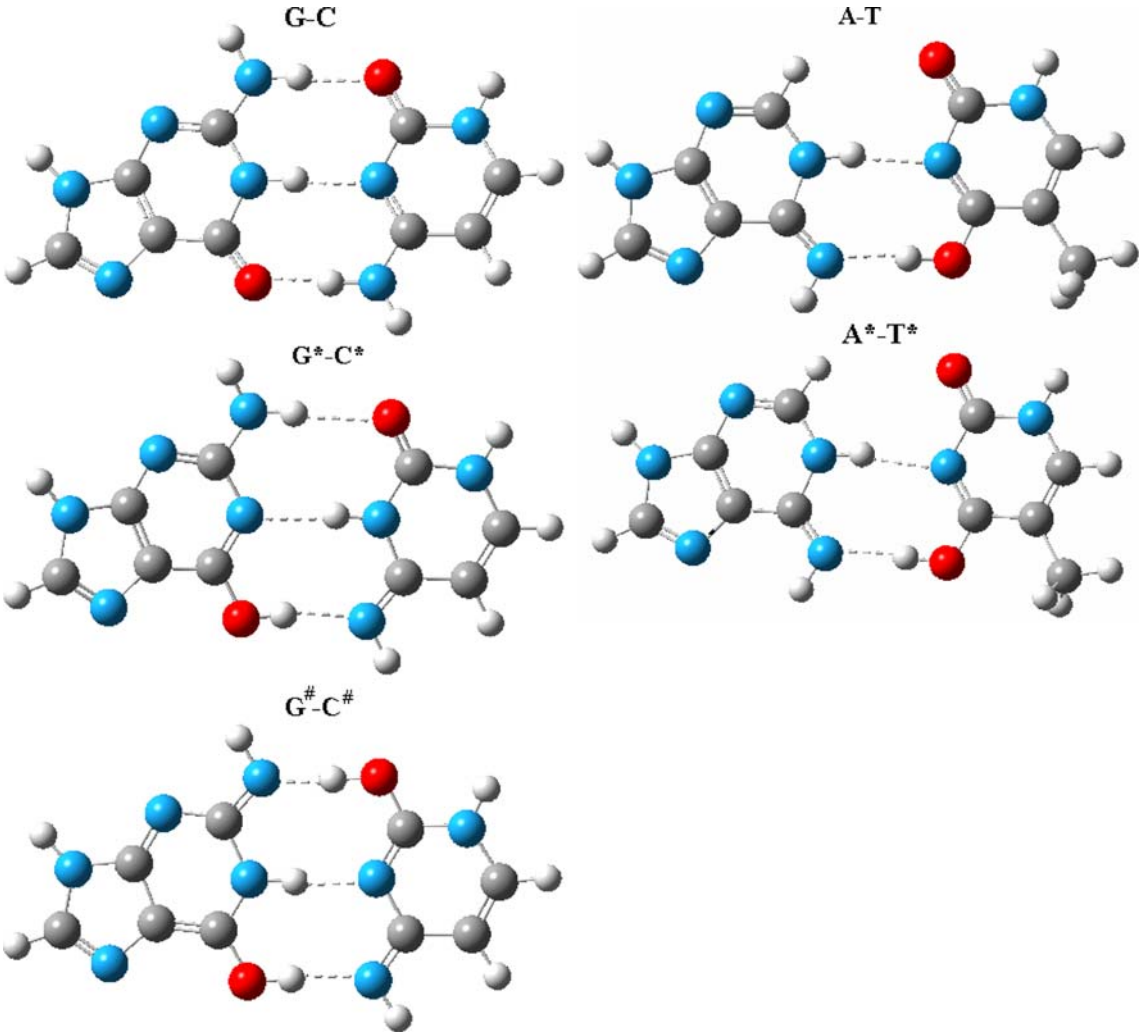

Fig. 4 The main tautomers of the guanine–cytosine and adenite–thymine base pairs

change more easily. The same different behavior in the hydrogen bridges can be found in the guanine–cytosine system: the N–H–N and the O–H–N bonds are *soft* and the N–H–O bond is *hard* (Fig. 5). This difference in the behavior of the hydrogen bridges is not due to the intrinsic characteristic of these bonds, since it disappears when the other coordinates not directly involved in the hydrogen bridges are frozen.

We have found that the suitable mechanism for the conversion of A–T to A*–T* cannot be a concerted double hydrogen transfer. Only a two-step mechanism is possible, since the movement of hydrogen in the N–O bridge is frozen, when the hydrogen in the other hydrogen bridge is around the equilibrium position of the A–T structure. Instead, the change of energy due to the movement of hydrogen in the N–N bridge is softer. The two-step mechanism of A*–T* formation is not efficient and

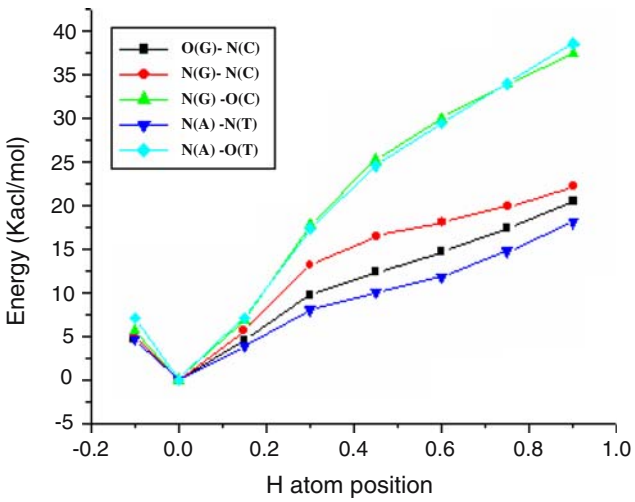

Fig. 5 Energy curves as a function of the hydrogen position

only a small amount of this tautomer can be found at any time; nevertheless, it generates several hundreds of mutation points in a DNA with a million A–T (or T–A) bases (Fig. 6). Apart from these two tautomers, and in larger amount than the A*–T* structure, the dynamical $A^{\delta+} - T^{\delta-}$ tautomer results from the transfer of hydrogen atom in the N–N bridge from thymine to adenine [39]. Instead, the suitable mechanism for the conversion of G–C to G*–C* can be both the concerted double hydrogen transfer and the two-step process, since these two hydrogen bonds are *soft* according to our nomenclature. On the contrary, the G–C to $G^{\#}$–$C^{\#}$ conversion is mainly a two-step process, since one bridge is *hard* and the other is *soft*. The amount of these tautomers is in any case sufficient to generate several thousands of mutation points in the G*–C* structure and hundreds in the $G^{\#}$–$C^{\#}$ structure in DNA with one million of G–C (or C–G) bases (Fig. 7). Beyond these three tautomers, there are the dynamical $G^{\delta+}$–$C^{\delta-}$ and $G^{\delta-}$–$C^{\delta+}$

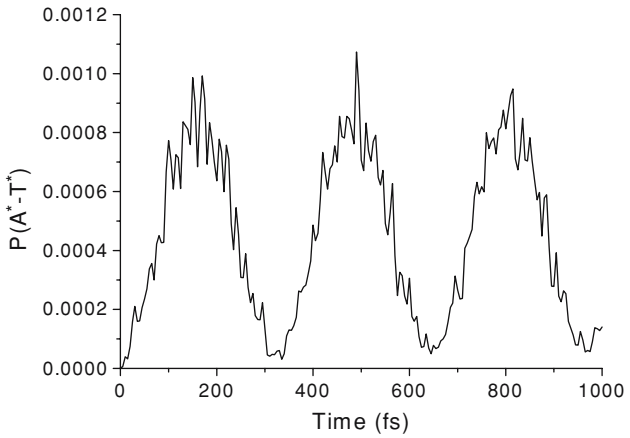

Fig. 6 Time-dependent probability of the A*–T* tautomer

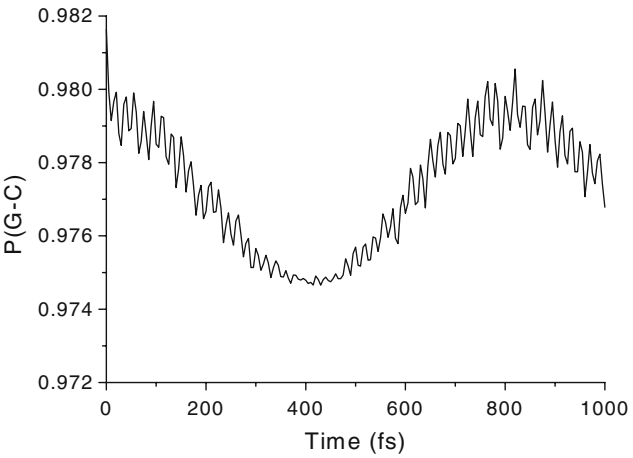

Fig. 7 Time-dependent probability of the G–C tautomer

tautomers (not reported here) [40], related to the transfer of hydrogen atom in the N—O, N—N and O—N bridges, i.e. from guanine to cytosine and vice versa. It is noteworthy that the probabilities of the imino-enol tautomers of both adenine–thymine and guanine–cytosine presented here have been computed from the TDSE, while in the literature static thermal populations are usually found.

The consequence of the significant amount of the so-called rare tautomer populations and of their time evolution on biological properties can be summarized as follows. First of all, there is a large difference between these quantum probabilities and the frequency of spontaneous mutations since the value [43] of this frequency in DNA is from 10^{-8} to 10^{-10}. Of course, we must also remember that the rate of spontaneous mutation is related to the biological condition: for example, the occurrence of mutations in the non-replicated genome is significantly slower than the one taking place during DNA replication [44]. In any case, we believe that this large difference can be an indication of a minor role of the base pair tautomerisation in the mutation process. Second, the difference in stability between A–T and G–C has been related [45] to the deficiency of the G–C content of the DNA in higher organisms [46], which is generally as low as 0.5 times (0.4 in humans) the A–T content. We believe that also this consideration is not reasonable, since our calculation supports the same stability for the A–T and G–C systems. Finally, it is worthwhile to recall that our studies show, for the first time, a periodic behavior of the imino-enol structures to be compared with the non-periodic behavior of the imino-enol-imino-enol $G^{\#}$–$C^{\#}$ tautomer (also exhibiting large variations in the amount of these structures). It is interesting to mention that the simultaneous occurrence of opposite behaviors in the same system is one of the most intriguing results in the area of Complexity Science.

Looking at the atomic charge variation during these processes of hydrogen transfer, one may notice that this is not a simple proton transfer. The hydrogen atomic charge changes through the transfer from the donor to the acceptor, but one cannot say that the *bare* proton moves while the electron remains in the original fragment. The process of hydrogen transfer in the base pairs systems must instead be regarded as a proton-coupled electron transfer [47,48]. Moreover, in both cases, the heavy atoms supporting the bridge have complementary charge variations with the acceptor becoming less negative and the donor more negative.

In [34] we have studied the relation between the hydrogen atoms transfer and the base stacking interaction. Two phenomena are present in the polynucleotide system: the stacking coupling among a base pair and its

neighbors and the dynamical process of hydrogen atoms' transfer in the base pair. These two, phenomena interact since the base–base stacking coupling is modified by the hydrogen atoms passage from the complementary bases in a pair. Of course, this modification is maximum for the nearer bases and decrease in farther bases. Hence we assume that only the nearer bases are coupled to a specific base in the chain. These modifications are time dependent since the process of hydrogen transfer is time-dependent and a simple sinusoidal behaviour is assumed.

The base stacking energy consists of two parts. The van der Waal's component of stacking is overlap-dependent and includes the dominating dispersion attraction as well as steric effects. The electrostatic component of stacking reflects the mutual interaction of molecular electrostatic potentials of bases. In contrast to the variable electrostatic stacking terms, the van der Waal's contributions are essentially independent of the sequence. Their total values are highly conserved, ranging from -16.6 to -16.9 kcal/mol [49]. There are moderate variations in the Pyr-Pyr and Pur-Pyr(3′) terms, correlated with the presence or absence of the N2-amino group. In addition to the base–base interactions, it would be possible to analyze other contributions to the potential energy as well, e.g., sugar–base interactions. However, the interbase interactions most probably contain the majority of stacking coupling effects.

The main result of this study [34] can be considered to be the evidence of a longtime coherent process of complete transfer of hydrogen atoms in a base pair in the condition of consecutive identical base pairs. In this case, the amount of the so-called "rare tautomers," the imino-enol tautomeric forms of DNA base pairs, can become much larger, until the complete passage, in the oligomer systems.

4 Conclusions

The examples discussed in the previous two sections well illustrate the usefulness of a time-dependent approach in quite different research areas. Among the many other problems that have been studied with the help of a numerical propagation of wave-packets, we mentioned many examples in the field of theoretical photochemistry. These concern the systematic study of the dynamics around a conical intersection [20,41,50–52] and a recent contribution, in collaboration with the Olivucci group, focused on a new explanation for the observed multi-exponential decay of the retinal chromophore [53]. As a final remark, we want to mention that our future activity will be mainly focused on the development of methods for including more degrees of freedom in the calculations and for taking into account the role of the solvent in the dynamics of excited states.

References

1. Davis MJ, Heller EJ (1981) J Chem Phys 75:246
2. Heller EJ (1975) J Chem Phys 62:1544
3. Heller EJ (1981) Acc Chem Res 14:368
4. Van Vleck JV (1928) Proc Nat Acad Sci USA 14:178
5. Miller WH (2001) J Phys Chem A 105:2942
6. Herman MF, Kluk E (1984) Chem Phys 91:27
7. Köppel H, Cederbaum LS, Domcke W (1988) J Chem Phys 85:5805
8. Lami A, Villani G (1990) J Phys Chem 94:6959
9. Lami A, Villani G (1993) Chem Phys 172:285
10. Ferretti A, Lami A, Villani G (1993) Chem Phys 196:447
11. Meyer H-D, Manthe U, Cederbaum LS (1990) Chem Phys Lett 165:73
12. Manthe U, Meyer H-D, Cederbaum LS (1992) J Chem Phys 97:3199
13. Beck H, Jäckle A, Worth GA, Meyer H-D (2000) Phys Rep 324:1
14. Ferretti A, Lami A, Villani G (2000) Chem Phys 259:201
15. Bennet CH, Wiesner SJ (1992) Phys Rev Lett 69:2881
16. Grover LK (1997) Phys Rev Lett 79:325
17. Grover LK (1997) Phys Rev Lett 79:4709
18. Ahn J, Weinact TC, Bucksbaum PH (2000) Science 287:463
19. Giulini D, Joos E, Kiefer C, Kupsch J, Stamatescu I-O, Zeh HD (1996) Decoherence and the appearance of a classical world in quantum theory. Springer, Berlin Heidelberg New York
20. Lami A, Villani G (2004) In: Domcke W, Yarkony DR, Köppel H (eds) Conical intersections. World Scientific, Singapore, p 369 and references therein
21. Lami A (2001) In: Bloembergen N, Rahman NK, Rizzo A (eds) Atoms, molecules and quantum dots in laser fields, Italian Physical Society Conference Proceedings vol 171, p 145, and references therein
22. Rice SA, Zhao M (2000) Optical control of molecular dynamics. Wiley-Interscience, New York
23. Shapiro M, Brumer P (2000) In: Bederson B, Walther H (eds) Advances in atomic, molecular and optical physics, vol 42. Academic, San Diego, p 287
24. Weiner AM, Leaird DE, Patel JS, Wull JR (1990) Opt Lett 15:326
25. Judson RS, Rabitz H (1992) Phys Rev Lett 68:1500
26. Assion A, Baumert T, Bergt M, Brixner T, Kiefer B, Seyfried W, Strehle M, Gerber G (1998) Science 282:919
27. Lami A, Santoro F (2002) Chem Phys 277:297
28. Lami A, Santoro F (2003) Chem Phys 287:237
29. Lami A, Santoro F (2004) Chem Phys Lett 384:86
30. Lami A, Santoro F (2004) In: Becker W, Fedorov MV (eds) Universality and diversity in science. World Scientific, Singapore, p 97
31. Rabitz H, Zhu W (2000) Acc Chem Res 33:572
32. Zoete V, Meuwly M (2004) J Chem Phys 121:4377
33. Ivanov V, Zeng Y, Zocchi G (2004) Phys Rev E 70:51907
34. Villani G, Chem Phys (in press)
35. Löwdin PO (1963) Rev Mod Phys 35:724
36. Löwdin PO (1965) Adv Quantum Chem 2:213
37. Watson JD, Crick FHC (1953) Nature 171:737 and 964

38. Florián J, Hrounda V, Hobza P (1994) J Am Chem Soc 116:1457
39. Villani G (2005) Chem Phys 316:1
40. Villani G (2006) Chem Phys 324:438
41. Ferretti A, Granucci G, Lami A, Persico M, Villani G (1996) J Chem Phys 104:5517
42. Hamilton IP, Light JC (1986) J Chem Phys 84:306
43. Bacic Z, Light JC (1986) J Chem Phys 85:4594
44. Nir E, Plützer C, Kleinermanns K, de Vries MS (2002) Eur Phys J D 20:317
45. Auerbach C (1976) Mutation reaserch, problems, results and perspectives. Wiley, New York
46. Florián J, Leszczyński J (1996) J Am Chem Soc 118:3010
47. Komberg A, Baker T (1992) DNA Replication. W. H. Freeman, New York
48. Villani G (2002) J Chem Phys 117:1279
49. Villani G (2004) Chem Phys 302:309
50. Lankas F, Cheatham III TE, Špač ková N, Hobza P, Langowski J, Šponer J (2002) Biophys J 82:2592
51. Ferretti A, Lami A, Villani G (1997) J Chem Phys 106:934
52. Ferretti A, Lami A, Villani G (1997) J Chem Phys 107:3948
53. Ferretti A, Lami A, Villani G (1998) J Chem Phys 109:9002
54. Olivucci M, Lami A, Santoro F (2005) Angew Chem Int Ed 44:5118